MISSOURI S&T

Missouri University of Science and Technology

Scholars' Mine

Physics Faculty Research & Creative Works

Physics

01 Nov 2009

Nuclear Form Factor, Validity of the Equivalent Photon Approximation and Coulomb Corrections to Muon Pair Production in Photon-Nucleus and Nucleus-Nucleus Collisions

Ulrich D. Jentschura
Missouri University of Science and Technology, ulj@mst.edu

V. G. Serbo

Follow this and additional works at: https://scholarsmine.mst.edu/phys_facwork

Part of the Physics Commons

Regular Article - Theoretical Physics

Nuclear form factor, validity of the equivalent photon approximation and Coulomb corrections to muon pair production in photon–nucleus and nucleus–nucleus collisions

U.D. Jentschura[1,2], V.G. Serbo[2,3,a]

[1]Department of Physics, Missouri University of Science and Technology, Rolla, MO 65409-0640, USA
[2]Institut für Theoretische Physik, Universität Heidelberg, Philosophenweg 16, 69120 Heidelberg, Germany
[3]Novosibirsk State University, Pirogova 2, 630090 Novosibirsk, Russia

Abstract We study in detail the influence of the nuclear form factor both on the Born cross section and on the Coulomb corrections to the photo-production of muon pairs off heavy nuclei ($\gamma Z \to \mu^+\mu^- Z$) and in heavy-ion collisions ($ZZ \to ZZ\mu^+\mu^-$). Our findings indicate a number of issues which have not been sufficiently described as yet in the literature: (i) the use of a realistic form factor, based on the Fermi charge distribution for the nucleus, is absolutely indispensable for reliable theoretical predictions; (ii) we checked quantitatively that the equivalent photon approximation has a very good accuracy for the discussed processes; and (iii) we present a leading logarithmic calculation of the Coulomb corrections which correspond to multi-photon exchange of the produced $\mu^\pm$ with the nuclei. These corrections are found to be small (on the percent level). Our result justifies using the Born approximation for numerical simulations of the discussed process at the RHIC and LHC colliders. Finally, we calculate the total cross section for muon pair production at RHIC and LHC.

1 Introduction

Lepton pair production in ultra-relativistic nuclear collisions was discussed in numerous papers (see [1–3] for a review and references therein). For definiteness, we restrict ourselves to equal charge numbers of the nuclei $Z_1 = Z_2 \equiv Z$ and symmetric Lorentz factors $\gamma_1 = \gamma_2 \equiv \gamma$, for the RHIC and the LHC colliders with parameters given in Table 1.

In the present paper, we primarily consider the production of a muon pair, but for completeness and comparison, we first recall some results for electron–positron (e^+e^-) pair

production and therefore make a slight detour. The production of a single e^+e^- pair in the Born approximation is described by the Feynman diagram of Fig. 1; the corresponding cross section was obtained many years ago [4, 5]. Since the Born cross section $\sigma_{\text{Born}}^{e^+e^-}$ is huge (see Table 1), the e^+e^- pair production can be a serious background for many experiments. It is also an important issue for the beam lifetime and luminosity of these colliders [6]. This means that various corrections to the Born cross section, as well as the cross section for n-pair production, are of great importance. The subject is inherently difficult; a number of controversial and incorrect statements in the literature have been clarified in Refs. [1, 7–11].

Since the parameter $Z\alpha$ is not small ($Z\alpha \approx 0.6$ for Au–Au and Pb–Pb collisions), the whole series in $Z\alpha$ has to be summed in order to obtain the cross section with sufficient accuracy unless higher-order corrections are otherwise parametrically suppressed. The exact cross section for single pair production σ_1 can be represented as the sum of the Born value, the Coulomb correction, and of the unitarity correction,

$$\sigma_1 = \sigma_{\text{Born}} + \sigma_{\text{Coul}} + \sigma_{\text{unit}}. \tag{1}$$

The Coulomb correction σ_{Coul} corresponds to multi-photon exchange of the produced $e^\pm$ with the nuclei (Fig. 2); it was calculated in Refs. [7, 11]. The unitarity correction σ_{unit} corresponds to the exchange of light-by-light blocks

Table 1 Cross sections for the production of light lepton pairs at modern colliders

Collider	Z	γ	$\sigma_{\text{Born}}^{e^+e^-}$ [kb]	$\sigma_{\text{Born}}^{\mu^+\mu^-}$ [b]
RHIC, Au–Au	79	108	36.0	0.209
LHC, Pb–Pb	82	3000	227	2.46

[a]e-mail: serbo@math.nsc.ru

310

Eur. Phys. J. C (2009) 64: 309–317

between the nuclei (Fig. 3); it was calculated in [9, 10]. It was found that the Coulomb corrections are about 10% while the unitarity corrections are about two times smaller (see Table 2). In the last column of Table 2 is shown the result of Baltz (see Ref. [12]) obtained by numerical calculations using formula for the cross section resulting from "exact solution of the semiclassical Dirac equations." In fact, the employed formulas allow to calculate the Coulomb correction in the leading logarithmic approximation only, and this may account for the discrepancies of the results for RHIC indicated in Table 2. For the case of electron–positron pairs, the leading logarithmic approximation is insufficient because of the large absolute magnitude of the correction.
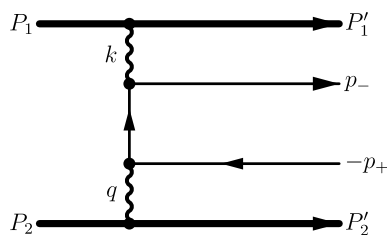

Fig. 1 Feynman diagram for the lepton pair production $ZZ \to ZZl^+l^-$ in the Born approximation ($l = e, \mu$)
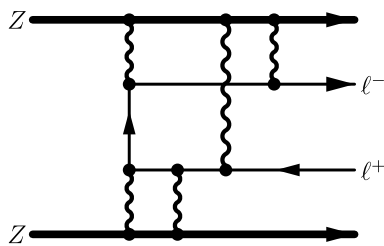

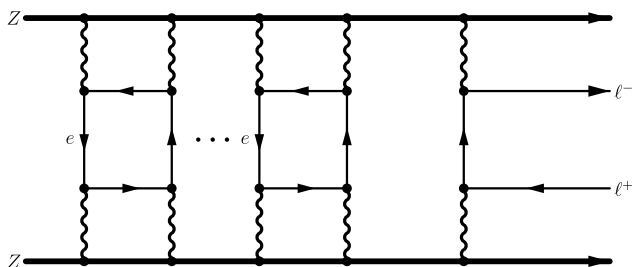**Fig. 2** Feynman diagram for the Coulomb correction

Fig. 3 Feynman diagram for the unitarity correction

In this paper, we present detailed calculations related to muon pair production. This process may be easier to observe experimentally than e^+e^- pair production. It should be stressed that the calculational scheme, as well as, the final results for the $\mu^+\mu^-$ pair production are quite different from those for the e^+e^- pair production.

The principal issues related to muon pair production, including the problem of unitarity corrections, have been considered in Refs. [10, 13]. In particular, using simple estimates, it was pointed out that: (i) the Born contribution can be easily calculated using the equivalent photon approximation (EPA) which has in our particular case a good accuracy; (ii) contrary to the e^+e^- case, the Coulomb correction is small in the muon case (on the level of a percent). The last statement is of principal importance because it justifies the validity of the Born approximation for event generators of this process at the RHIC and LHC colliders.

In a recent paper [14], the conclusion (i) has been confirmed, but the point (ii) has been questioned. Namely, in Ref. [14], it was found out that the Coulomb corrections to muon pair production are rather large: -22% for RHIC and -17% for LHC. These results have been obtained using the same formulas as for the e^+e^- case with the minor changes. Below, we present a new calculation of the Coulomb corrections for muon pair production in the leading logarithmic approximation (LLA); our result is in agreement with a previous numerically small estimate of the Coulomb corrections as given in Ref. [13], but it is in strong disagreement with the result of Ref. [14].

We would like to note that the above features (i) and (ii) are directly related to the fact that both the electromagnetic form factors of the nuclei $F(K^2)$, $F(Q^2)$ and the cross section for the virtual block $\gamma^*(k) + \gamma^*(q) \to \mu^+\mu^-$ drop quickly with increasing photon virtualities $K^2 = -k^2 > 0$ and $Q^2 = -q^2 \approx \boldsymbol{q}^2 > 0$. However, the scale of this decrease is much less for the nuclear form factor than for the virtual $\gamma^* + \gamma^* \to \mu^+\mu^-$ block (by γ^*, we here denote a virtual as opposed to a real photon).

As a rule, the calculation of muon pair production for nuclear collisions is very laborious (for example, the exact expression for the Born cross section even for the case of simplified form factors is an eight-fold integral). Therefore, it is convenient to check the main points of various approximations using the simpler process of muon photo-production. In this case we have a possibility to perform relatively easily both the exact and approximate calculations and compare them.

Collider	$\frac{\sigma_{Coul}}{\sigma_{Born}}$ (Refs. [7, 11])	$\frac{\sigma_{unit}}{\sigma_{Born}}$ (Refs. [9, 10])	$\frac{\sigma_{Coul}}{\sigma_{Born}}$ (Ref. [12])
RHIC, Au–Au	-10%	-5.0%	-17%
LHC, Pb–Pb	-9.4%	-4.0%	-11%

Table 2 Coulomb and unitarity corrections to the e^+e^- pair production

This paper is organized as follows. In Sect. 2, we study in detail the photo-production of muon pair off heavy nuclei $\gamma Z \to \mu^+ \mu^- Z$. An exact calculation of the total Born cross section for arbitrary photon energy starting from the threshold is carried out. The use of a realistic form factor instead of simplified form $F(Q^2) = 1/(1 + Q^2/\Lambda^2)$ turns out to be critically important for moderate photon energies. In Sect. 3, the validity of the EPA is studied both for a realistic and for a simplified representation of the nuclear form factor. Coulomb corrections to photo-production of the muon pair are studied in Sect. 4. Predictions for the RHIC and LHC colliders are given in Sect. 5, and we conclude with a summary in Sect. 6. Throughout the paper, we use a system of units in which $c = 1$, $\hbar = 1$, $\alpha = e^2/(\hbar c) \approx 1/137$ and denote the muon and nuclear mass m and M, respectively.

2 Form factor and Born-level pair photo-production

2.1 Form factors and nuclear charge distributions

We first recall basic formulas related to the realistic and simplified form factor representations for the colliding heavy nuclei which are central to our investigation. For the realistic form factor, we employ a Fermi-type nuclear charge distribution in the form (see Refs. [15, 16])

$$\rho(r) = \frac{\rho_0}{1 + \exp[(r - R)/a]} \qquad (2)$$

with $a = 2.30/(4 \ln 3)$ fm, $R = 6.55$ fm for Au (mass number $A = 197$) and $R = 6.647$ fm for Pb ($A = 208$). This leads to the mean squared radius

$$\sqrt{\langle r^2 \rangle} = \sqrt{\frac{3}{5}\left[1 + \frac{7}{3}\left(\frac{\pi a}{R}\right)^2\right]} R, \qquad (3)$$

with $\sqrt{\langle r^2 \rangle} = 5.4338$ fm for gold and $\sqrt{\langle r^2 \rangle} = 5.5041$ fm for lead. The latter numbers are in very good agreement with the experimental values $\sqrt{\langle r^2 \rangle}_{\mathrm{exp}} = 5.4358$ fm for gold and $\sqrt{\langle r^2 \rangle}_{\mathrm{exp}} = 5.5010$ fm for lead.

The nuclear form factor is defined as

$$F(\boldsymbol{q}^2) = \frac{1}{N} \int \rho(r) e^{-i\boldsymbol{q} \cdot \boldsymbol{r}} d^3r, \qquad N = \int \rho(r) d^3r, \qquad (4)$$

where $\boldsymbol{q}^2 \approx Q^2$ and $\boldsymbol{q}$ is the three-vector part of the photon four-momentum q. Its behavior is shown on Fig. 4, it is seen that for $Q^2 > 1/R^2$, the form factor drops quickly with the growth of Q^2. On the other hand, the cross section for the virtual block $\gamma^* + \gamma^* \to \mu^+ \mu^-$ drops quickly with the growth of Q^2 at $Q^2 > W^2 = (k + q)^2 > (2m)^2$ [see (19) below]. For further consideration it is important that

$$1/R^2 \approx (30\ \mathrm{MeV})^2 \ll W^2. \qquad (5)$$

For *the simplified form factor*, we use an approximation of a monopole form factor corresponding to an exponen-
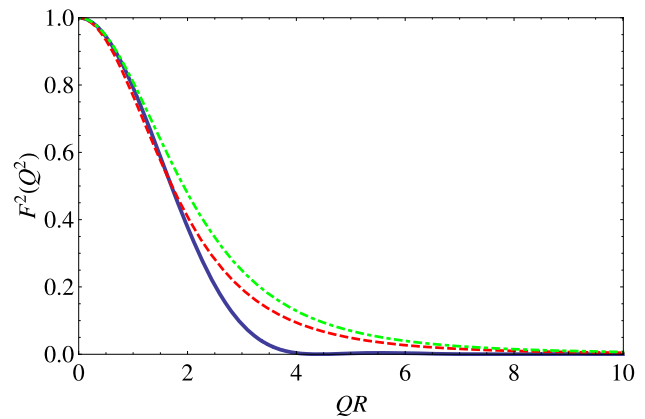

Fig. 4 Realistic (*solid line*) and simplified (*dashed line* for $\Lambda = 80$ MeV and *dot-dashed line* for $\Lambda = 90$ MeV) form factors vs. QR for Au

tially decreasing charge distribution

$$F(Q^2) = \frac{1}{1 + Q^2/\Lambda^2}. \qquad (6)$$

Its behavior is also shown in Fig. 4. This approximate form of the form factor is used, for example, in Refs. [13, 14, 17] and enables to perform some calculations analytically. For the concrete calculations reported in Refs. [13, 14], the value

$$\Lambda = 80\ \mathrm{MeV} \qquad (7)$$

is used for lead and gold. In the calculations below we also use this value unless otherwise stated. Another possibility is to use the connection of Λ with the mean squared radius $\sqrt{\langle r^2 \rangle}$; in this case

$$\Lambda = \sqrt{\frac{6}{\langle r^2 \rangle}} \approx 90\ \mathrm{MeV} \qquad (8)$$

for lead and gold.

Looking at three curves in Fig. 4, one can come to the conclusion that the difference between the two choices of the Λ parameter should be negligible. We will show, however, that a transition from the realistic form factor to the simplified one with $\Lambda = 80$ MeV or $\Lambda = 90$ MeV results in a change of the total cross section for the muon pair production at the RHIC collider on the level of 10% or 20%, respectively.

2.2 Realistic form factor: exact result for the Born cross section

We start to discuss the role of the form factor on the basis of muon pair production by a real photon with the energy ω off the nucleus with charge Ze and mass M:

$$\gamma(k) + Z(P) \to \mu^+(p_+) + \mu^-(p_-) + Z(P'). \qquad (9)$$

312

Eur. Phys. J. C (2009) 64: 309–317

In the Born approximation, this process is described by the Feynman diagram of Fig. 5, and the corresponding diagram is also contained as a block diagram within the Feynman diagram for pair production off heavy nuclei. We assume that a real photon with 4-momentum k and a virtual photon with 4-momentum $q = P - P'$ and virtuality

$$Q^2 = -q^2 > 0 \tag{10}$$

collide with each other and produce a $\mu^+\mu^-$ pair with the invariant mass squared

$$W^2 = (k + q)^2 = 2kq - Q^2. \tag{11}$$

We also use the notation

$$s = (k + P)^2 = M^2 + 2\omega M, \qquad \sigma_0 = \frac{Z^2 \alpha^3}{m^2}, \tag{12}$$

where m is the muon mass. So, ω measures the incoming photon energy in the rest frame of the incoming nucleus.

The exact cross section for muon pair production $\sigma_{\gamma Z}$ can be split into the form

$$\sigma_{\gamma Z} = \sigma_{\text{Born}} + \sigma_{\text{Coul}}, \tag{13}$$

where σ_{Born} corresponds to the Born cross section, and the Coulomb correction σ_{Coul} corresponds to multi-photon exchange of the produced $\mu^\pm$ with the nucleus (Fig. 6).

It is well known (see, for example, Ref. [18]) that the exact Born cross section for the process (1) as well
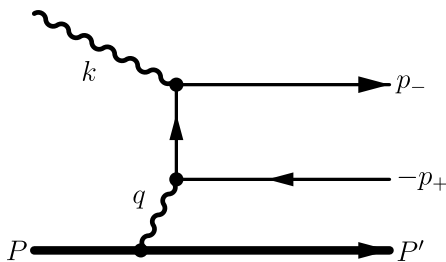
Fig. 5 Feynman diagram for the photo-production of muon pair in the Born approximation. The incoming virtual photon has momentum k, the invariant mass squared of the pair is $W^2 = (k+q)^2 = (p_+ + p_-)^2$. The four-momenta of the produced leptons are $p_\pm$
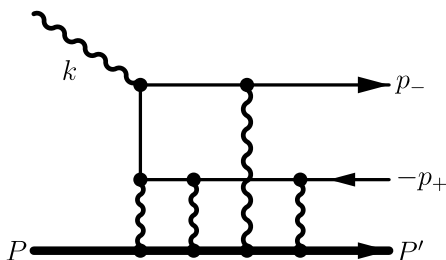
Fig. 6 Typical Feynman diagram for a higher-order Coulomb correction to the photo-production of a muon pair

as for electro-production can be written in terms of two structure functions or two cross sections $\sigma_T(W^2, Q^2)$ and $\sigma_S(W^2, Q^2)$ for the virtual processes $\gamma\gamma_T^* \to \mu^+\mu^-$ and $\gamma\gamma_S^* \to \mu^+\mu^-$, respectively (here, γ is a real initial photon, while γ_T^* and γ_S^* denote the virtual transverse and scalar/longitudinal photons with helicity $\lambda_T = \pm 1$ and $\lambda_S = 0$, respectively):

$$d\sigma_{\text{Born}} = \sigma_T(W^2, Q^2) \, dn_T(W^2, Q^2) + \sigma_S(W^2, Q^2) \, dn_S(W^2, Q^2). \tag{14}$$

The coefficients dn_T and dn_S are called the number of transverse and scalar virtual photons (generated by the nucleus). The cross sections σ_T and σ_S can be found in Appendix E of the review [18]:

$$\sigma_T = \frac{4\pi\alpha^2}{W^2 + Q^2} \left\{ \left[1 + \frac{4m^2W^2 - 8m^4 - 2Q^2W^2}{(W^2 + Q^2)^2} \right] L - \left[1 + \frac{4m^2W^2 - 4Q^2W^2}{(W^2 + Q^2)^2} \right] v \right\}, \tag{15}$$

$$\sigma_S = \frac{16\pi\alpha^2 Q^2 W^2}{(W^2 + Q^2)^3} \left[v - \frac{2m^2}{W^2} L \right], \tag{16}$$

where

$$v = \sqrt{1 - \frac{4m^2}{W^2}}, \qquad L = 2\ln\left[\frac{W}{2m}(1 + v) \right]. \tag{17}$$

Let us note that

$$\sigma_T \sim \frac{4\pi\alpha^2}{W^2}\left[1 + \mathcal{O}(Q^2/W^2)\right],$$
$$\sigma_S \sim \frac{16\pi\alpha^2 Q^2}{W^4} \quad \text{at } Q^2 \ll W^2, \tag{18}$$

and

$$\sigma_T \sim \frac{4\pi\alpha^2}{Q^2}, \qquad \sigma_S \sim \frac{16\pi\alpha^2 W^2}{(Q^2)^2} \quad \text{for } Q^2 \gg W^2. \tag{19}$$

The number of photons can be found in Sect. 6 and Appendix D of Ref. [18]

$$dn_T = \frac{Z^2\alpha}{\pi}\left(1 - y - \frac{M^2 y^2}{Q^2}\right) F^2(Q^2) \frac{dW^2}{W^2 + Q^2} \frac{dQ^2}{Q^2},$$
$$dn_S = \frac{Z^2\alpha}{\pi}\left(1 - y + \frac{1}{4}y^2\right) F^2(Q^2) \frac{dW^2}{W^2 + Q^2} \frac{dQ^2}{Q^2}, \tag{20}$$

where

$$y = \frac{kq}{kP} = \frac{W^2 + Q^2}{2\omega M}. \tag{21}$$

Integrating the cross section (14) over Q^2 in the region $Q^2_{\min} \leq Q^2 \leq Q^2_{\max}$, where (see Problem 3 to §68 in
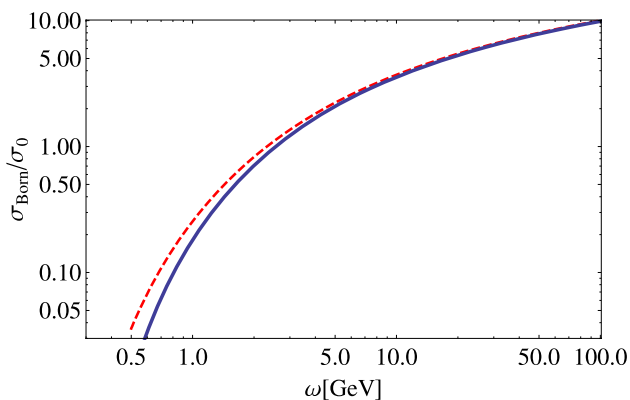
Fig. 7 Born cross section for the realistic (*solid line*) and simplified (*dashed line*) form factors (photo-production on Au)

Ref. [19])

$$Q^2_{\min,\max} = B \mp \sqrt{B^2 - C}, \tag{22}$$

$$2B = \frac{2M^6 - M^4 W^2 - M^2 W^4}{(2M^2 + W^2)s} + s - 2M^2 - W^2$$

$$\approx 2\frac{2\omega^2 - W^2(1 - \omega/M)}{1 + 2\omega/M}, \tag{23}$$

$$C = \frac{M^2 W^4}{s}, \tag{24}$$

and over W in the region $2m \leq W \leq \omega$, we obtain the exact result for the Born cross section presented in Fig. 7.

2.3 Simplified form factor: exact result for the Born cross section

The exact result for the Born cross section for the case of a simplified form factor can be obtained using (14), (15), (16), (20) with the form factor (6). The result is shown by the dashed line in Fig. 7. It is seen that calculations with the simplified form factor give an accuracy better than 10%, 5% and 2% at $\omega > 3.5$ GeV, 8 GeV and 50 GeV, respectively. At RHIC, the region near the "accuracy threshold" ($2m < \omega < 8$ GeV) gives a numerically important contribution, which accounts for about 10–20% of the difference between cross sections with the realistic and simplified form factors.

3 Approximations to Born-level pair photo-production

3.1 Realistic form factor: equivalent photon approximation (EPA)

Let us recall the usual schema of the EPA, but with the addition of an accurate treatment of the nuclear form factor (see,

for example, Ref. [18]). For the case of high-energy photons $\omega \gg 2m$, the most important contribution to the photo-production cross section stems from photons with very small virtuality $Q^2 \ll W^2$ [we recall the definition of ω in (12) and that $Q^2 = -q^2 \approx \boldsymbol{q}^2$]. It means that we can ignore the contribution of the scalar photons in (14) and the dependence of σ_T on Q^2; besides we can simplify the expression for dn_T from (20). As a result, we obtain the simple approximate (EPA) expression

$$d\sigma_{\text{Born}}^{\text{EPA}} = \sigma_{\gamma\gamma}(W^2)\, dn_\gamma(W^2, Q^2), \tag{25}$$

where

$$\sigma_{\gamma\gamma}(W^2) = \frac{4\pi\alpha^2}{W^2}\left[\left(1 + \frac{4m^2}{W^2} - \frac{8m^4}{W^4}\right)L\right.$$
$$\left. - \left(1 + \frac{4m^2}{W^2}\right)v\right], \tag{26}$$

$$dn_\gamma = \frac{Z^2\alpha}{\pi}\left(1 - \frac{Q^2_{\min}}{Q^2}\right)F^2(Q^2)\frac{dW^2}{W^2}\frac{dQ^2}{Q^2},$$

$$Q^2_{\min} = \frac{W^4}{4\omega^2}. \tag{27}$$

The quantities v and L are defined in (17).

Integrating this spectrum over Q^2, we obtain (the upper limit of this integration can be set to be equal to infinity in a good approximation, due to the fast convergence of the integral at $Q^2 > 1/R^2$):

$$dn_\gamma(W^2) = \frac{Z^2\alpha}{\pi}f\left(\frac{W^2 R}{2\omega}\right)\frac{dW^2}{W^2}. \tag{28}$$

The function

$$f(x) = \int_{x^2}^{\infty}\left(1 - \frac{x^2}{y}\right)F^2\left(\frac{y}{R^2}\right)\frac{dy}{y} \tag{29}$$

is presented in Fig. 8. It is large for small values of x,

$$f(x) = \ln\left(\frac{1}{x^2}\right) - C_0 \quad \text{for } x \ll 1. \tag{30}$$

(The value of constant C_0 depends slightly on the ratio a/R: we obtain $C_0 = 0.166$ for gold and $C_0 = 0.163$ for lead.) However, $f(x)$ drops very quickly for large x,

$$f(x) < \frac{1}{x^4} \quad \text{for } x > 1. \tag{31}$$

Finally we obtain

$$\sigma_{\text{Born}}^{\text{EPA}} = \frac{Z^2\alpha}{\pi}\int_{4m^2}^{\infty}\frac{dW^2}{W^2}f\left(\frac{W^2 R}{2\omega}\right)\sigma_{\gamma\gamma}(W^2). \tag{32}$$

A comparison of this cross section with the exact result is shown in Fig. 9. It is seen that the EPA gives an accuracy
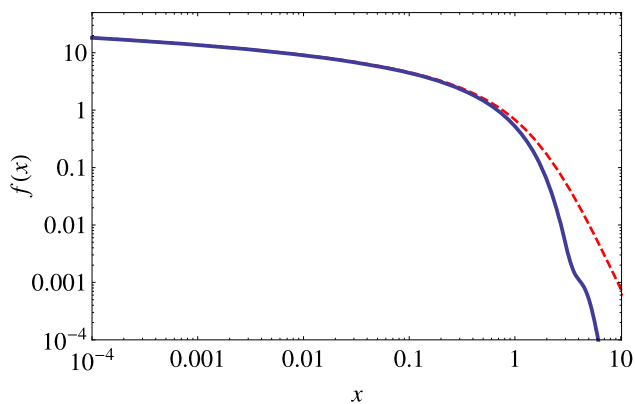
Fig. 8 The function $f(x)$ from (29) for the realistic form factor (*solid line*) and $\tilde{f}(x/(R\Lambda))$ from (36) for the simplified form factor (*dashed line*) (photo-production on Au)
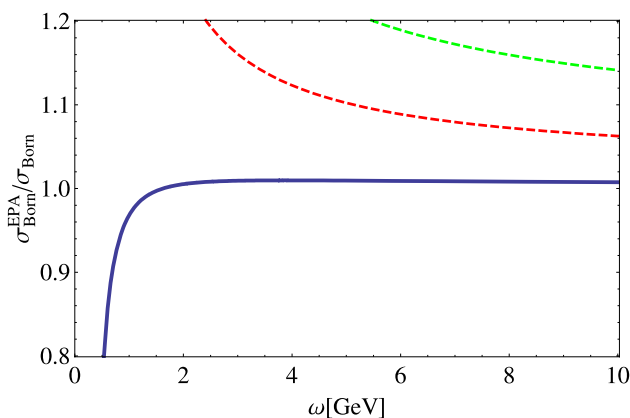

Fig. 9 Ratio $\sigma_{\text{Born}}^{\text{EPA}}/\sigma_{\text{Born}}$ (*solid line*) and $\sigma_{\text{Born}}^{\text{SEPA}}/\sigma_{\text{Born}}$ (*dashed and dash-dotted lines*), where σ_{Born} is the total Born cross section from (14) while $\sigma_{\text{Born}}^{\text{EPA}}$ from (32) is calculated for the case of realistic form factor and $\sigma_{\text{Born}}^{\text{SEPA}}$ from (39) is calculated for the case of a simplified form factor with $\Lambda = 80$ MeV (*dashed line*) and $\Lambda = 90$ MeV (*dash-dotted line*) (photo-production on Au)

better than 1% already at $\omega > 1.3$ GeV. This needs to be explained.

Going from the exact expressions (14), (15), (16), (20) to the approximate ones (25), (26), (28) we omit terms of the relative order of Q^2/W^2, which are dropped before the integration over Q^2 is done. After the integration with the "weight function" $F^2(Q^2)/Q^2$ the relative value of these corrections becomes of the order of $1/(R^2W^2)$. In addition, the contribution of these correction terms is suppressed by a logarithmic factor. Indeed, the main contribution to the cross section in EPA is proportional to the large Weizsäcker–Williams logarithm

$$L_{\text{WW}} = \int_{Q_{\text{min}}^2}^{1/R^2} \frac{dQ^2}{Q^2} \approx 2\ln\left(\frac{\omega}{2m^2R}\right), \tag{33}$$

while the omitted terms have no such logarithm. Therefore, the actual parameter describing the suppression of the omitted terms to the differential cross section for pair production is numerically small indeed,

$$\eta_{\text{EPA}} \sim \frac{1}{R^2W^2L_{\text{WW}}}. \tag{34}$$

3.2 Simplified form factor: EPA

The replacement of the realistic by the simplified form factor means that we have to replace the function f from (29) by a function $\tilde{f}$ which is obtained when we replace the form factor in the integrand in (29) appropriately by the simplified nuclear form factor. The SEPA (S here stands for the simplified form factor) can thus be obtained using (25) and (26) with the following expression for the number of equivalent photons:

$$dn_\gamma(W^2) = \frac{Z^2\alpha}{\pi}\tilde{f}\left(\frac{W^2}{2\omega\Lambda}\right)\frac{dW^2}{W^2}. \tag{35}$$

The function $\tilde{f}[W^2/(2\omega\Lambda)]$ can be obtained analytically,

$$\tilde{f}(\tilde{x}) = \left(1 + 2\tilde{x}^2\right)\ln\left(\frac{1}{\tilde{x}^2} + 1\right) - 2. \tag{36}$$

This is in contrast to $f(x)$, which would be the equivalent of $\tilde{f}(\tilde{x})$ for a realistic form factor [see (29)]. Now, $\tilde{f}(\tilde{x})$ is large for small values of $\tilde{x}$,

$$\tilde{f}(\tilde{x}) \approx \ln\left(\frac{1}{\tilde{x}^2}\right) - 2 \quad \text{for } \tilde{x} \ll 1, \tag{37}$$

but drops very quickly for large $\tilde{x}$:

$$\tilde{f}(\tilde{x}) < \frac{1}{6\tilde{x}^4} \quad \text{for } \tilde{x} > 1. \tag{38}$$

Its behavior is presented by the dashed line in Fig. 8, where $x = R\Lambda\tilde{x}$. In view of the same leading logarithmic asymptotics for small argument [see (30) and (37)], the functions f and $\tilde{f}$ almost coincide for small values of x.

Finally, we obtain for the simplified equivalent photon approximation (SEPA),

$$\sigma_{\text{Born}}^{\text{SEPA}} = \frac{Z^2\alpha}{\pi}\int_{4m^2}^{\infty}\frac{dW^2}{W^2}\tilde{f}\left(\frac{W^2}{2\omega\Lambda}\right)\sigma_{\gamma\gamma}(W^2)$$
$$= \sigma_0 J(\omega\Lambda/m^2). \tag{39}$$

For large photon energies, the function $J(\omega\Lambda/m^2)$ behaves as

$$J(z) = \frac{28}{9}\left[\ln(z) - \frac{57}{14}\right] \quad \text{for } z \gg 1. \tag{40}$$

A comparison of SEPA cross section with the exact result from (14) is shown by the dashed and dot-dashed lines in Fig. 9. It is seen that the EPA gives a considerable better accuracy than the SEPA, once again confirming that the use of a realistic nuclear form factor is essential.

3.3 Realistic form factor: asymptotics for the Born cross section

The high-energy asymptotic behavior of the Born cross section (for a realistic form factor) at large $\omega \gg 2m$ can easily be obtained using the EPA formulas (25), (26), (28) with the asymptotic form of the function $f(x)$ given in (30). The final result is

$$\sigma_{\text{Born}}^{\text{asymp}} = \frac{28}{9}\sigma_0\left[\ln\left(\frac{2\omega}{Rm^2}\right) - \frac{43}{14} - \frac{1}{2}C_0\right]. \tag{41}$$

It should be noted that the cross section (41) provides a reasonable approximation only for large enough values of the photon energy ω. Indeed, this cross section is positive only at

$$\omega > \omega_{\text{crit}} = \frac{1}{2}Rm^2\exp\left(\frac{43}{14} + \frac{1}{2}C_0\right) = 4.4 \text{ GeV}. \tag{42}$$

A comparison of the asymptotics with the exact Born cross section is given in Fig. 10. It is seen that the accuracy of a simple expression (41) is better than 10% only at very large $\omega > 20$ GeV, showing that the realm of applicability of the high-energy asymptotics is limited.

3.4 Simplified form factor: result of Ivanov and Melnikov for asymptotics

The cross section $\sigma_{\gamma Z}$ in the high-energy limit was calculated by Ivanov and Melnikov in Ref. [17] using the same
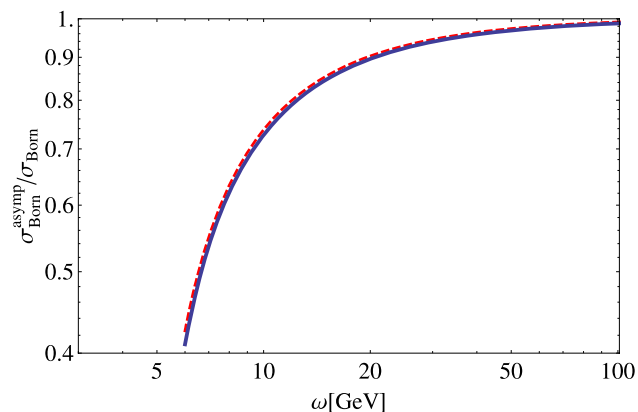

Fig. 10 Ratio $\sigma_{\text{Born}}^{\text{asymp}}/\sigma_{\text{Born}}$ for the realistic form factor (*solid line*) and ratio $\sigma_{\text{Born}}^{\text{IM}}/\sigma_{\text{Born}}$ (*dashed line*) (photo-production on Au)

expression (6) for the form factor of the nucleus and assuming $\Lambda^2/(2m)^2 \ll 1$. The corresponding analytical formula including the first correction $\sim \Lambda^2/(2m)^2$ reads

$$\sigma_{\gamma Z}^{\text{IM}} = \sigma_{\text{Born}}^{\text{IM}} + \sigma_{\text{Coul}}^{\text{IM}}, \tag{43}$$

$$\sigma_{\text{Born}}^{\text{IM}} = \frac{28}{9}\sigma_0\left[\ln\left(\frac{2\omega\Lambda}{m^2}\right) - \frac{57}{14} - C_1\right], \tag{44}$$

$$\sigma_{\text{Coul}}^{\text{IM}} = -\frac{28}{9}\sigma_0 C_2, \tag{45}$$

where

$$C_1 = \frac{12}{35}\left(\frac{\Lambda}{2m}\right)^2, \qquad C_2 = 0.928(Z\alpha)^2 C_1. \tag{46}$$

We note that the parameter $\Lambda^2/(2m)^2 = 0.14$ is small for muon pairs. A comparison of $\sigma_{\text{Born}}^{\text{IM}}$ with the exact Born cross section (14) is shown by dashed line in Fig. 10.

Two final remarks: (i) the SEPA asymptotics (40) is in accordance with the result of Ivanov and Melnikov (44), as has already been noted in [17]. (ii) The difference between the high-energy asymptotics $\sigma_{\text{Born}}^{\text{asymp}}$ for the realistic form factor (41) as opposed to the high-energy asymptotics $\sigma_{\text{Born}}^{\text{IM}}$ for a simplified form factor is very small:

$$\sigma_{\text{Born}}^{\text{IM}} - \sigma_{\text{Born}}^{\text{asymp}} = 0.012\frac{28}{9}\sigma_0. \tag{47}$$

This is not surprising because the asymptotics are determined by a region with small values of $x = W^2 R/(2\omega)$, in which the spectra of the equivalent photons for the realistic and simplified form factors coincide (see Fig. 8).

4 Coulomb correction to the photo-production of pairs

Having discussed the role of the nuclear form factor in the determination of the lepton pair production amplitude in the Born approximation, we now turn our attention to the role of Coulomb corrections. This is done according to our "master equation" (13). The Coulomb correction is the leading correction beyond the Born amplitude, provided the latter is being evaluated with exact form factors.

The Coulomb correction corresponds to Feynman diagram of Fig. 6. The calculation of the Coulomb correction for high photon energies ($\omega \gg 2m$) can be performed approximately using the result of Ivanov and Melnikov given in (45). The ratio $\sigma_{\text{Coul}}^{\text{IM}}/\sigma_{\text{Born}}$ as presented at Fig. 11 is small. It is seen that the relative magnitude of the Coulomb correction is less than 1% at $\omega > 20$ GeV. This is in accordance with the following estimate [13, 17].

Due to the restriction of the transverse momenta of additionally exchanged photons to the range below $\Lambda \sim 1/R$, the
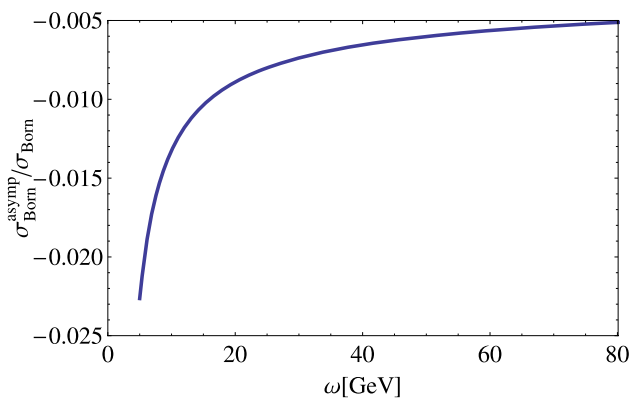
Fig. 11 Relative magnitude of the Coulomb correction (photo-production on Au)

effective parameter of the perturbation series is not $(Z\alpha)^2$ but

$$(Z\alpha)^2 \frac{\Lambda^2}{W^2}, \tag{48}$$

where W is the invariant mass of the muon pair. Besides, there is an additional logarithmic suppression because the Coulomb corrections lack the large Weizsäcker–Williams logarithm. Therefore, the actual parameter describing the relative value of the Coulomb correction is

$$\eta_{\text{Coul}} = (Z\alpha)^2 \frac{\Lambda^2}{W^2 L_{\text{WW}}} \tag{49}$$

which corresponds to Coulomb corrections of less then 1% for $\omega > 20$ GeV [we recall that L_{WW} is defined in (33)]. It is reassuring that the result of Ivanov and Melnikov confirms this estimate. Indeed the relative order of the Coulomb correction according to (44)–(46) is

$$\frac{\sigma_{\text{Coul}}^{\text{IM}}}{\sigma_{\text{Born}}^{\text{IM}}} = 0.318(Z\alpha)^2 \left(\frac{\Lambda}{2m}\right)^2 \left[\ln\left(\frac{2\omega\Lambda}{m^2}\right) - \frac{57}{14} - C_1\right]^{-1}$$

$$\sim \eta_{\text{Coul}}. \tag{50}$$

5 Predictions for the RHIC and LHC colliders

We now turn our attention to the muon pair production in collisions of heavy nuclei. Let us therefore consider the process

$$Z(P_1) + Z(P_2) \rightarrow \mu^+(p_+) + \mu^-(p_-) + Z(P_1') + Z(P_2'). \tag{51}$$

Its cross section can be calculated with a high accuracy by means of the EPA using the result (14) for the exact cross section of the process,

$$\gamma(k) + Z(P_2) \rightarrow \mu^+(p_+) + \mu^-(p_-) + Z(P_2'). \tag{52}$$

For the RHIC collider, we use the parameters $Z = 79$ and $\gamma = 100$, the latter in order to be accordance with the value used in Ref. [14]. In the Born (B) approximation and with a realistic (Fermi, F) form factor, we have

$$\sigma_{\text{BF}}^{ZZ} = \frac{Z^2\alpha}{\pi} \int_{2m}^{\infty} \frac{d\omega}{\omega} f\left(\frac{\omega R}{\gamma_L}\right) \sigma_{\text{Born}}^{\gamma Z}(\omega) = 0.193 \text{ barn.} \tag{53}$$

In (53), $\gamma_L = 2\gamma^2$ is the Lorentz factor of the first nucleus in the rest frame of the second nucleus; $f(x)$ and $\sigma_{\text{Born}}^{\gamma Z}(\omega)$ can be found in (29) and (14), respectively. There is a 9.8% difference to the corresponding result for the simplified (S) form factor, still in the first Born approximation,

$$\sigma_{\text{BS}}^{ZZ} = 0.212 \text{ barn.} \tag{54}$$

This is in full agreement with the recent result 0.211 barn of Ref. [14]. The consistent use of $\Lambda = 80$ is crucial in order to obtain this agreement. We note in passing that $\Lambda = 90$ MeV results in a 22% difference.

A calculation for the Coulomb correction in LLA can be done using the result of Ivanov–Melnikov and taking into account Coulomb corrections to both nuclear lines (factor 2),

$$\sigma_{\text{Coul}}^{ZZ} = \frac{Z^2\alpha}{\pi} \int_{2m}^{\infty} \frac{d\omega}{\omega} f\left(\frac{\omega R}{\gamma_L}\right) 2\sigma_{\text{Coul}}^{\text{IM}} = -0.0072 \text{ barn.} \tag{55}$$

It means that the relative value of the Coulomb correction is -3.7% in full contrast to the recent result -22% of Ref. [14], but in agreement with our parametric estimates.

For the LHC collider, we use $Z = 82$, $\gamma = 2760$, again in order to be in accordance with Ref. [14]. We have for a realistic form factor

$$\sigma_{\text{BF}}^{ZZ} = 2.36 \text{ barn,} \tag{56}$$

and for a simplified form factor

$$\sigma_{\text{BS}}^{ZZ} = 2.45 \text{ barn.} \tag{57}$$

This is in good agreement with the recent result 2.42 barn of Baltz [14]. Again, an estimate for the Coulomb correction can be obtained on the basis on an integration over the result of Ivanov and Melnikov,

$$\sigma_{\text{Coul}}^{ZZ} = -0.03 \text{ barn.} \tag{58}$$

It means that the relative value of the Coulomb correction is -1.3% in full contrast to the recent result -14% of Baltz [14].

For completeness, we recall that in Table 1, slightly different values were used for the relativistic Lorentz factors at the modern colliders, namely, $\gamma = 108$ (RHIC) and

$\gamma = 3000$ (LHC) instead of $\gamma = 100$ (RHIC) and $\gamma = 2760$ (LHC). In both cases, with the alternative values for γ and for a realistic nuclear form factor, we obtain results for σ_{BF}^{ZZ} which are slightly larger than those in (53) and (56), namely 0.209 barn for RHIC and 2.46 barn for the LHC (see Table 1).

6 Conclusions

We have analyzed in detail the role of the nuclear form factor in the calculation of muon pair production cross sections in photon–nucleus and nucleus–nucleus collisions. At RHIC, the realistic (Fermi) nuclear charge distribution leads to predictions that deviate by 10–20% from the corresponding values for simplified nuclear form factors. We also show quantitatively that the EPA is an excellent approximation to the muon photo-production for photon energies that exceed the rest mass of the produced pair (region $\omega \gg 2m$) as well as for muon pair production at RHIC and LHC.

We find that the Coulomb corrections for the muon production are less pronounced than for the e^+e^- pair production. Our calculation in LLA leads to a decrease by about 1.3–3.7% due to higher-order Coulomb effects at the LHC and RHIC colliders.

Let us issue a few remarks regarding the obvious discrepancy of our results about the Coulomb corrections to those of the recent, interesting paper [14]. It is not obvious from the condensed presentation given in Ref. [14] whether or not the nuclear form factors have been taken into account to all orders in $Z\alpha$. Therefore, the approach may need to be re-examined. Moreover, our parametric quantitative estimates given by the numerically small expansion parameter (49) indicate that the Coulomb corrections for muon pair production should be smaller than those for e^+e^- production. Coulomb corrections for the total production cross section of heavier lepton pairs would be even smaller, and in addition, we note that the Coulomb corrections also decrease with higher invariant mass W^2. Under typical conditions, muons from the discussed process can be detected at the RHIC and LHC colliders with large values of W; this means that the Born approximation can be safely used in numerical simulations of this process. A correction on the order of 22% for muons at RHIC, as obtained in Ref. [14], is larger than that for the e^+e^- production and seems unrealistically large even if we allow for a large numerical prefactor multiplying the parameter (49). We also note that the calculation of the Coulomb corrections in Ref. [14] proceeds in the impact parameter representation. The numerical evaluation of integrals of this type is known to be notoriously problematic because of large numerical cancellations due to oscillations. In any case, a calculation of the Coulomb corrections beyond the leading logarithmic approximation is desirable.

Finally, it should be mentioned than unitarity corrections to the muon production have been discussed in Refs. [10, 13] with the following result: unitarity corrections for the exclusive production of exactly one muon pair are large. However, the experimental study of the exclusive muon pair production seems to be a very difficult task, because it requires that the muon pair should be registered without any electron–positron pair production, including $e^{\pm}$ emitted at very small angles. The corresponding inclusive cross section is not affected by the unitarity correction and, indeed, close to the Born cross section.

Note added in proof

We were informed by Professor W. Schäfer that in the paper M. Klusek, W. Schäfer and A. Szczurek (Phys. Lett. B **674**, 92 (2009)) the necessity to use a realistic nuclear form factor for the description of ρ^0–ρ^0 production at RHIC also has been discussed.

References

1. G. Baur, K. Hencken, D. Trautmann, S. Sadovsky, Yu. Kharlov, Phys. Rep. **364**, 359 (2002)
2. G. Baur, K. Hencken, D. Trautmann, Phys. Rep. **453**, 1 (2007)
3. A. Baltz et al., Phys. Rep. **458**, 1 (2008)
4. L.D. Landau, E.M. Lifshitz, Phys. Z. Sow. **6**, 244 (1934)
5. G. Racah, Nuovo Cimento **14**, 93 (1937)
6. S.R. Klein, Nucl. Instrum. Methods A **459**, 51 (2001). arXiv:physics/0005032
7. D.Yu. Ivanov, A. Schiller, V.G. Serbo, Phys. Lett. B **454**, 155 (1999)
8. R.N. Lee, A.I. Milstein, Phys. Rev. A **61**, 032103 (2000)
9. R.N. Lee, A.I. Milstein, V.G. Serbo, Phys. Rev. A **65**, 022102 (2002)
10. U.D. Jentschura, K. Hencken, V.G. Serbo, Eur. Phys. J. C **58**, 281 (2008)
11. R.N. Lee, A.I. Milstein, arXiv:0903.0235 [hep-ph]
12. A. Baltz, Phys. Rev. C **71**, 024901 (2005). arXiv:nucl-th/0409044
13. K. Hencken, E.A. Kuraev, V.G. Serbo, Phys. Rev. C **75**, 034903 (2007)
14. A. Baltz, arXiv:0901.0891 [nucl-th]
15. G. Fricke et al., At. Data Nucl. Data Tables **60**, 177 (1995)
16. I. Angeli, At. Data Nucl. Data Tables **87**, 185 (2004)
17. D. Ivanov, K. Melnikov, Phys. Rev. D **57**, 4025 (1998)
18. V.M. Budnev, I.F. Ginzburg, G.V. Meledin, V.G. Serbo, Phys. Rep. **15C**, 181 (1975)
19. V.B. Berestetskii, E.M. Lifshitz, L.P. Pitaevskii, *Quantum Electrodynamics*, 2nd edn. (Pergamon, New York, 1994)